

taneously (AND operation). The polarization of the VCSEL is changed from 0° to 90° by the reset pulses. The 2.5 Gbits/s demultiplexed output signals are selected once every 40 bits from the 100 Gbits/s optical input signal.

1. H. Kawaguchi, *Bistabilities and Nonlinearities in Laser Diodes* (Artech House, Norwood, Mass., 1994).
2. H. Kawaguchi, I.H. White, M.J. Offside, J.E. Carroll, *Opt. Lett.* **17**, 130 (1992).
3. H. Kawaguchi, I.S. Hidayat, Y. Takahashi, Y. Yamayoshi, *Electron. Lett.* **31**, 109 (1995).
4. H. Kawaguchi, I.S. Hidayat, *Electron. Lett.* **31**, 1150 (1995).
5. T. Yoshikawa, H. Kosaka, K. Kurihara, M. Kajita, Y. Sugimoto, K. Kasahara, *Appl. Phys. Lett.* **66**, 908 (1995).

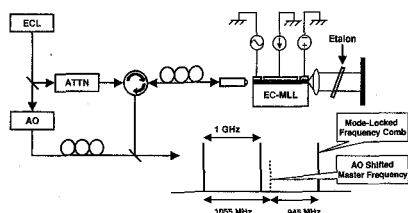
CThr2 2:45 pm

Phase coherence and frequency control of a hybrid mode-locked semiconductor laser by cw optical injection locking

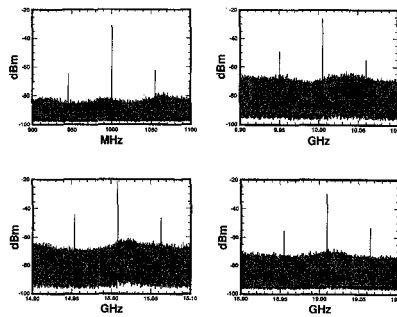
Thomas Jung,* Ji-Lin Shen, Dennis T.K. Tong, Ming C. Wu, Robert Lodenkamper,* Larry Lembo,* Michael Wickham,* Richard Davis,* John C. Brock,* Tawee Tanbun-Ek,** *UCLA, Electrical Engineering Department, Los Angeles California*

Mode-locked lasers have many versatile signal-processing applications. However, frequency control and phase coherence of the mode-locked laser optical frequency comb is often needed to make these applications possible, as in channelizer applications. We extend the principle of optical injection locking of cw lasers to optical injection locking of mode-locked semiconductor lasers¹⁻³ to establish phase coherence and frequency control. This method allows us to phase lock an entire comb of frequencies to a single frequency source. Compared to pulsed injection locking of mode-locked semiconductor lasers,⁴ cw injection locking to mode-locked semiconductor lasers offers added simplicity but does not synchronize the timing of the pulses of the mode-locked laser.

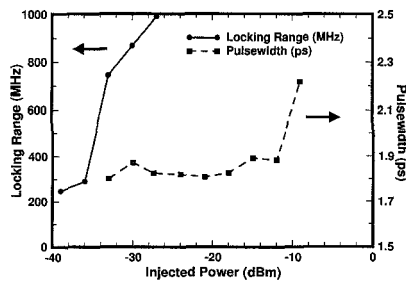
An external cavity hybrid mode-locked laser (EC-MLL) is constructed as shown in Fig. 1. A monolithic hybrid mode-locked semiconductor laser is antireflection coated on one facet and coupled to an external cavity. The external cavity length is 15 cm, which corresponds to a repetition rate of 1 GHz. An etalon with a 5-nm FWHM is placed in the external cavity to prevent mode-locking in clusters² and for tunability. The EC-MLL can be tuned



CThr2 Fig. 1. Injection locking mode-locked laser setup.



CThr2 Fig. 2. Heterodyne tone centered at 1, 10, 15, and 19 GHz.



CThr2 Fig. 3. Locking range and pulsewidth vs. injected power.

over 20 nm from 1540 to 1560 nm; pulsewidths <2.5 ps were achieved over the entire tuning range and were ~1.6 times the transform limit. An external cavity laser (ECL) is used as the master laser, its output is attenuated then injected into the mode-locked slave laser via an optical circulator. Part of the master laser is frequency shifted by 55 MHz using an acousto-optic frequency shifter for heterodyne detection. Injection locking of the EC-MLL is verified when tones at 945 and 1055 MHz appear. These tones are due to the heterodyne of the adjacent modes of the EC-MLL with the frequency shifted master laser (Fig. 1) and can be observed up to an instrument-limited 19 GHz (Fig. 2).

The locking range is measured by monitoring the offset frequency of the master laser at which the tones disappear (Fig. 3). Similar to injection locking of two cw lasers, the locking range is shown to increase with injected powers. Injected power levels well below the average power of the hybrid mode-locked laser show little effect on the pulsewidth (Fig. 3). At injection powers comparable to the average power of the EC-MLL (-9 dBm), the pulsewidth broadens significantly and the autocorrelation trace shows a significant increase in substructure. The pulse-broadening effect is due to the additional optical dc bias on the saturable absorber, which reduces the pulse-sharpening effect.

In conclusion, we have demonstrated phase coherence between a cw single-wavelength master laser and a multiwavelength mode-locked slave laser by optical injection locking.

This project is supported in part by TRW, Inc., and Rome Laboratory.

*TRW, Photonics Technology Department

**Bell Laboratories, Lucent Technologies

1. F. Mogensen, H. Olesen, G. Jacobsen, *IEEE J. Quantum Electron.* **21**, 784-93 (1985).
2. L.G. Joneckis, P.T. Ho, G. Burdge, *IEEE J. Quantum Electron.* **27**, 1854-1858 (1991).
3. M. Teshima, M. Koga, K. Sato, *Opt. Lett.* **22**, 126-128 (1997).
4. M. Margalit, M. Orenstein, H.A. Haus, *IEEE J. Quantum Electron.* **32**, 155-160 (1996).

CThr3

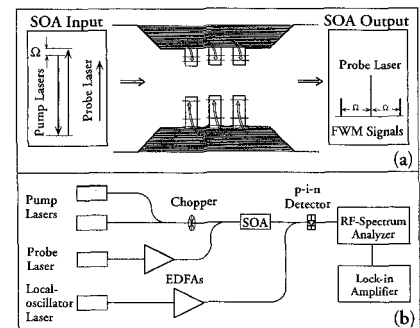
3:00 pm

Four-wave mixing mediated by the capture of carriers in semiconductor quantum-well amplifiers

Guido Hunziker, Roberto Paiella, Kerry J. Vahala, Uzi Koren,* *Department of Applied Physics, Mail Stop 128-95, California Institute of Technology, Pasadena, California 91125*

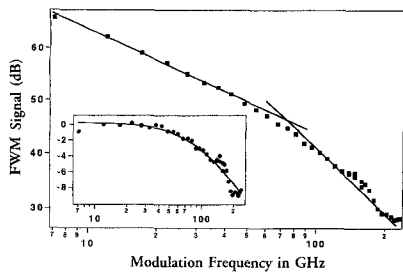
The capture and escape of charge carriers into and out of quantum wells (QWs) have been shown to affect the spectral and dynamic features of QW lasers. Measurements of the pertinent time constants often involve a compound response involving drift, diffusion, and energy relaxation along with the actual capture/escape processes. In this work, we demonstrate a technique to measure the intrinsic capture lifetime, using frequency-resolved four-wave mixing (FWM). The work is based on a frequency-domain measurement of the response function associated with the transfer of a modulation from three-dimensional states above the QW to the quantum-confined two-dimensional states.

The principle of the experiment is shown in Fig. 1. Two distributed feedback (DFB) lasers ($\lambda = 1.31 \mu\text{m}$) are combined with a probe at $\lambda = 1.54 \mu\text{m}$ and coupled into the active region of a semiconductor optical amplifier (SOA). Photomixing of the two pump waves at $1.3 \mu\text{m}$ generates a small signal modulation of the carrier density in the QW barrier states. This



CThr3 Fig. 1. Pictorial description of the experiment (a) and schematics of the experimental layout (b). The total pump power at 1.3 μm was 2 mW, and the probe power was 17 mW at the SOA input. The SOA was 780 μm long and biased at 100 mA. The DFB laser frequencies were adjusted by temperature control. To remove the frequency dependence of the rf electronics, the local oscillator was at a fixed detuning relative to the FWM signal. Lock-in detection was also used for improved sensitivity.

Thursday, May 7



CThR3 Fig. 2. Measured optical intensity of the FWM signal versus modulation frequency (the origin of the vertical axis is arbitrary). As emphasized by the continuous lines, the slope of the data changes from -20 to -40 dB/dec with increasing detuning frequency. The inset displays the same data with the initial 20 dB/dec roll-off subtracted; the continuous curve is a single-pole frequency response with pole at $88 \text{ GHz} = 1/(2\pi \times 1.8 \text{ ps})$.

modulation is then transferred to the QW states, where it creates a gain and refractive-index modulation. The probe wave is scattered by this transferred modulation, and the resulting FWM sidebands are measured as a function of pump detuning by optical heterodyne detection. This technique is similar to that described in Ref. 1, but by using optical photomixing of two pump waves combined with heterodyne detection of the FWM signal, we extend the measured frequency range by one order of magnitude to 230 GHz in this work. This is significant because our system measurement response encompasses the expected carrier capture corner frequency.

A typical FWM trace is shown in Fig. 2. The data exhibit a 20 dB/dec roll-off at low modulation frequencies (associated with the interband stimulated recombination of the carriers in the QWs) and a 40 dB/dec roll-off at modulation frequencies >90 GHz. The inset shows the same data but with the interband recombination 20 dB/dec roll-off normalized out. We can clearly identify another pole at ~ 88 GHz corresponding to a lifetime of 1.8 ps. The solid line in the inset shows a fit of the data to a two-pole frequency response, which is the result of a simple rate equation model.

Whereas the time constant inferred is consistent with the result of an earlier experiment using polarization-resolved FWM,² the fit is not adequate to explain the two shoulders appearing at 140 and 200 GHz that resemble the nulls of a phase-matching frequency response. A fit to a damped phase-matching response can reproduce these features, but the damping would correspond to only 10 dB of absorption for the pump waves at $1.3 \mu\text{m}$, whereas we measure losses in excess of 20 dB. Further experiments to resolve this issue using shorter-interaction-length SOAs (e.g., using lower barrier energies to increase the losses of the pump waves) are under consideration. With the data available to date, however, the time constant inferred should be regarded as an upper limit to the capture lifetime.

In conclusion, the results clearly indicate how the proposed technique can be used to measure the QW capture response, up to modulation frequencies larger than the expected capture rate. The technique is particu-

larly attractive because, provided that phase matching can be eliminated as a source of frequency dependence, the capture lifetime can be directly read off the data, as in the simple normalization carried out in the inset to Fig. 2.
*Lucent Technologies, Holmdel, New Jersey 07733

1. D. Vassilovski, T.C. Wu, S. Kan, K.Y. Lau, C.E. Zah, IEEE Photonics Technol. Lett. 7, 706 (1995).
2. R. Paiella, G. Hunziker, K.J. Vahala, U. Koren, Appl. Phys. Lett. 69, 4142 (1996).

CThR4 **3:15 pm**

Broadband spectral coupling in multiwavelength mode-locked semiconductor lasers

H. Shi, P.J. Delfyett, G.A. Alphonse, J.C. Connolly,* *Center for Research and Education in Optics and Lasers (CREOL), University of Central Florida, Orlando, Florida 32816; E-mail: delfyett@faculty.creol.ucf.edu*

Compact, efficient sources of ultrashort, high-repetition-rate optical pulses are of great interest in various applications, including nonlinear ultrafast signal processing, optical telecommunications, and medical imaging.

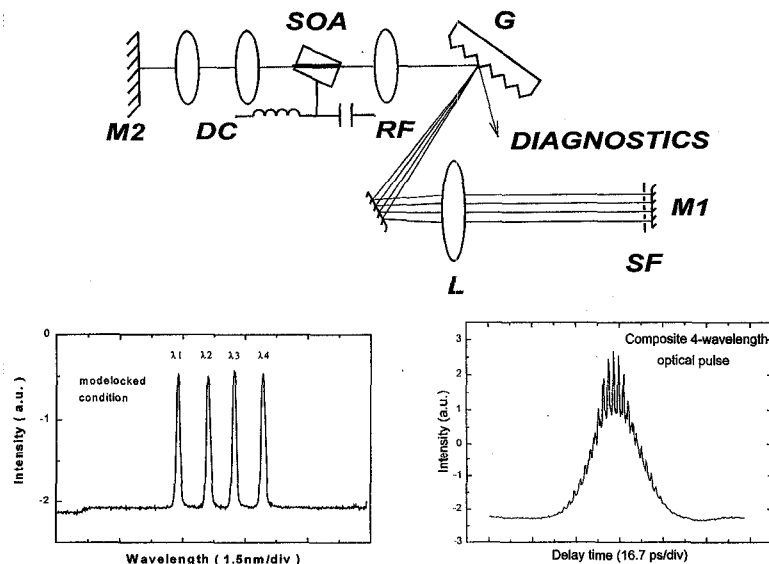
In this paper, we demonstrate broadband spectral coupling in a novel multiwavelength mode-locked semiconductor laser, which is capable of coherently coupling the spectral phases over a range of six times that of the normal active mode locking. The physical mechanism responsible for the broad range coupling is observed to be intracavity four-wave mixing generated by the dynamic carrier heating and cooling effects within the diode gain element.

The experimental configuration for generating coherently coupled four-wavelength output is shown in Fig. 1.¹ The output multiwavelength spectrum and the autocorrelation

trace of the resultant composite four-wavelength pulse are plotted in the inset of Fig. 1. The uniform spectral intensity of the four wavelengths demonstrates the robustness of multiwavelength generation from a diode laser under mode-locked operation. The intensity autocorrelation measures optical pulsewidth of 12 ps, with temporal modulation on the pulse envelop, which is inversely proportional to the frequency difference between adjacent wavelength channels.

To verify the possible phase correlation between the multiple wavelengths, a spectrogram of the multiwavelength output pulse is measured by using second-harmonic frequency resolved optical gate (FROG) methods.² In Fig. 2(a), the FROG trace shows seven stripes and significant modulation along the temporal delay. The seven stripes are a direct result of the convolution of spectra of two fields in the frequency domain, whereas the modulation is due to the difference in photon energy involved in the SHG process, e.g., $0, \Delta, 2\Delta$, and 3Δ , as can clearly be seen in the close-up FROG trace in Fig. 2(b). The correlated phase can be justified by the long-range modulation throughout the entire temporal delay and is also confirmed by theoretical FROG simulations.

Figure 3(a) is a spectrum of the four-wavelength mode-locked laser, showing the existence of FWM sidebands for wavelength channels with a frequency difference of $\Delta, 2\Delta$, and 3Δ . This suggests that there is energy exchange between each wavelength channel. To further clarify the energy exchange between each channel, the laser was operated with only two wavelengths with a frequency difference of Δ , the FWM sidebands were measured, and their frequency position noted, as shown in Fig. 3(b). From this figure, it is seen that all FWM sidebands lie within the bandwidth of the four mode-locked channels and serve as seeding mechanisms to assist in establishing a



CThR4 Fig. 1. Schematic of the experiment setup. SOA: semiconductor optical amplifier; G: grating (1800 lines/mm); SF: spatial filter; L: 150 mm achromatic lens; M: end mirrors. Left inset: optical spectrum of mode-locked four-wavelength diode laser. Right inset: intensity autocorrelation of the composite four-wavelength optical pulse.